Synthesis and Electrochemistry of Nickel and Cobalt Complexes of Mixed Thia–Aza Crown Ethers: Single-crystal Structures of $[Ni([18]aneN_2S_4)][PF_6]_2{\cdot}0.33H_2O$ and $[Co([18]aneN_2S_4)][PF_6]_3{\cdot}3H_2O$ ($[18]aneN_2S_4$ = 1,4,10,13-tetrathia-7,16-diazacyclooctadecane)†

Alexander J. Blake, Gillian Reid and Martin Schröder*
Department of Chemistry, The University of Edinburgh, West Mains Road, Edinburgh EH9 3JJ, UK

The mixed thia–aza donor macrocyclic complexes $[M([18]aneN_2S_4)]^{2+}$ (M = Ni or Co; $[18]aneN_2S_4$ = 1,4,10,13-tetrathia-7,16-diazacyclooctadecane) and $[Ni(Me_2[18]aneN_2S_4)]^{2+}$ ($Me_2[18]aneN_2S_4$ = 7,16-dimethyl-1,4,10,13-tetrathia-7,16-diazacyclooctadecane) were prepared by reaction of $M(NO_3)_2{\cdot}6H_2O$ with the appropriate crown ether in aqueous ethanol. The complex $[Ni([18]aneN_4S_4)][PF_6]_2{\cdot}0.33H_2O$ crystallises in the orthorhombic space group *Pcab* with a = 12.8260(20), b = 18.083(3), c = 22.200(4) Å and Z = 8. The structure shows the Ni^{II} encapsulated in a near-octahedral geometry, with the macrocycle adopting a *rac* configuration. Both diastereoisomeric forms of *rac*-$[Ni([18]aneN_2S_4)]^{2+}$ are present in the crystal structure in approximately 1:1 ratio. Aerial oxidation of $[Co([18]aneN_2S_4)][PF_6]_2$ in water afforded the corresponding cobalt(III) complex: $[Co([18]aneN_2S_4)][PF_6]_3{\cdot}3H_2O$ crystallises in the monoclinic space group $P2_1/n$ with a = 11.5485(3), b = 13.9779(2), c = 19.1378(4) Å, β = 106.561(2)° and Z = 4. The structure shows the Co^{III} bound to all six macrocyclic donors in a distorted-octahedral geometry. The ligand adopts a *rac* configuration around the metal centre. In both complexes there is a small but significant tetrahedral distortion of the four sulfur donors out of the best S_4 co-ordination plane. The complex $[Co([18]aneN_2S_4)][PF_6]_3{\cdot}3H_2O$ exhibits an extensive hydrogen-bonding network involving the macrocyclic cation, PF_6^- anions and H_2O solvent molecules. Electrochemical data, electronic and ESR spectroscopic data for the complexes are also discussed in the context of their donor sets and ligand configurations and conformations.

There is considerable interest in the metal-ion chemistry of aza and thia crown ethers.[1,2] Interest in such complexes has been stimulated by their unusual thermodynamic stability and kinetic inertness, and these are thought to be largely responsible for the rich electrochemical behaviour often observed. This has enabled stabilisation of rare oxidation states such as mononuclear Rh^{II}, Au^{II}, Ag^{II}, Pd^{I} and Pd^{III}.[1-5] We are particularly interested in establishing relationships between the stereochemical features of complexes, ligand conformations and their electronic and redox properties. The existence of weak, long-range M–S donor atom interactions as seen, for example, in the crystal structures of $[Pd([18]aneN_2S_4)]^{2+}$ ($[18]aneN_2S_4$ = 1,4,10,13-tetrathia-7,16-diazacyclooctadecane)[4] and $[Pd([9]aneS_3)_2]^{2+}$ ($[9]aneS_3$ = 1,4,7-trithiacyclononane)[5] has led to the stabilisation of mononuclear palladium(III) species. This approach has also enabled us to rationalise the very different redox behaviour observed for $[Pd([18]aneN_2S_4)]^{2+}$ and for the closely related $[Pd(Me_2[18]aneN_2S_4)]^{2+}$ cation ($Me_2[18]aneN_2S_4$ = 7,16-dimethyl-1,4,10,13-tetrathia-7,16-diazacyclooctadecane).[4]

We report herein the synthesis and redox properties of $[M([18]aneN_2S_4)]^{2+}$ (M = Ni or Co) and $[Ni(Me_2[18]aneN_2S_4)]^{2+}$. The single-crystal structures of $[Ni([18]aneN_2S_4)][PF_6]_2{\cdot}0.33H_2O$ and $[Co([18]aneN_2S_4)][PF_6]_3{\cdot}3H_2O$ are also reported.

Results and Discussion

Reaction of $Ni(NO_3)_2{\cdot}6H_2O$ with 1 molar equivalent of

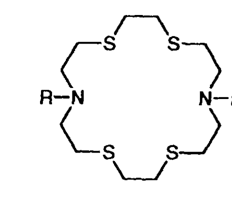

$[18]aneN_2S_4$ R = H
$Me_2[18]aneN_2S_4$ R = Me

$[18]aneN_2S_4$ or $Me_2[18]aneN_2S_4$ in refluxing aqueous EtOH, followed by addition of an excess of NH_4PF_6 and recrystallisation from MeCN, yields $[Ni([18]aneN_2S_4)][PF_6]_2$ or $[Ni(Me_2[18]aneN_2S_4)][PF_6]_2$ respectively in high yield. These formulations were confirmed by IR and electronic spectroscopy, FAB mass spectrometry $\{[Ni([18]aneN_2S_4)(PF_6)]^+$, *m/z* 529; $[Ni(Me_2[18]aneN_2S_4)(PF_6)]^+$, *m/z* 557$\}$, and by microanalytical data. In order to confirm the ligand configuration around the Ni^{II} a single-crystal X-ray determination on $[Ni([18]aneN_2S_4)][PF_6]_2{\cdot}0.33H_2O$ was undertaken. The structure shows (Fig. 1, Table 1) the Ni^{II} bound in an octahedral arrangement of all six macrocyclic donor atoms, Ni–S(1) 2.407(5), Ni–S(4) 2.430(5), Ni–S(10) 2.403(6), Ni–S(13) 2.416(7), Ni–N(7) 2.126(13) and Ni–N(16) 2.065(13) Å. The complex cation adopts the *rac* configuration, with the chelating S(4)–N(7)–S(10) and S(1)–N(16)–S(13) units linked in a *meridional* manner. This arrangement contrasts with the structure of the homoleptic thioether complex $[Ni([18]aneS_6)]^{2+}$ ($[18]aneS_6$ = 1,4,7,10,13,16-hexathiacyclooctadecane) which adopts a *meso* form, with compressed Ni–S bond lengths (*cf.* the sum of the

† *Supplementary data available:* see Instructions for Authors, *J. Chem. Soc., Dalton Trans.*, 1994, Issue 1, pp. xxiii–xxviii.

Table 1 Bond lengths (Å), angles and torsion angles (°) for $[Ni([18]aneN_2S_4)]^{2+}$

Ni–S(1)	2.407(5)	Ni–N(16)	2.065(13)	S(10)–C(9)	1.839(19)	N(7)–C(8)	1.408(23)
Ni–S(4)	2.430(5)	S(1)–C(2)	1.793(20)	S(10)–C(11)	1.853(23)	C(2)–C(3)	1.45(3)
Ni–S(10)	2.403(6)	S(1)–C(18)	1.830(13)	S(13)–C(12)	1.818(24)	C(5)–C(6)	1.51(3)
Ni–S(13)	2.416(7)	S(4)–C(3)	1.846(19)	S(13)–C(14)	1.830(15)	C(8)–C(9)	1.54(3)
Ni–N(7)	2.126(13)	S(4)–C(5)	1.814(19)	N(7)–C(6)	1.488(22)	C(11)–C(12)	1.50(3)
S(1)–Ni–S(4)	87.81(17)	S(10)–Ni–N(16)	97.2(4)	Ni–S(10)–C(11)	103.8(7)	Ni–N(16)–C(17′)	108.5(9)
S(1)–Ni–S(10)	92.91(19)	S(13)–Ni–N(7)	95.6(4)	C(9)–S(10)–C(11)	102.8(9)	C(15)–N(16)–C(17)	138.2(12)
S(1)–Ni–S(13)	170.4(2)	S(13)–Ni–N(16)	85.0(4)	Ni–S(13)–C(12)	103.6(8)	C(15′)–N(16)–C(17′)	143.3(12)
S(1)–Ni–N(7)	94.0(4)	N(7)–Ni–N(16)	178.3(5)	Ni–S(13)–C(14)	96.3(5)	S(1)–C(2)–C(3)	117.2(14)
S(1)–Ni–N(16)	85.4(4)	Ni–S(1)–C(2)	101.8(6)	C(12)–S(13)–C(14)	103.2(9)	S(4)–C(3)–C(2)	115.5(13)
S(4)–Ni–S(10)	168.1(2)	Ni–S(1)–C(18)	96.1(4)	Ni–N(7)–C(6)	110.0(10)	S(4)–C(5)–C(6)	111.3(12)
S(4)–Ni–S(13)	93.90(20)	C(2)–S(1)–C(18)	103.6(7)	Ni–N(7)–C(8)	113.3(10)	N(7)–C(6)–C(5)	110.4(14)
S(4)–Ni–N(7)	83.6(4)	Ni–S(4)–C(3)	101.2(6)	C(6)–N(7)–C(8)	111.4(13)	N(7)–C(8)–C(9)	112.7(15)
S(4)–Ni–N(16)	94.8(4)	Ni–S(4)–C(5)	97.7(6)	Ni–N(16)–C(15)	111.6(9)	S(10)–C(9)–C(8)	110.9(12)
S(10)–Ni–S(13)	87.37(21)	C(3)–S(4)–C(5)	101.5(8)	Ni–N(16)–C(15′)	108.1(9)	S(10)–C(11)–C(12)	115.1(16)
S(10)–Ni–N(7)	84.4(4)	Ni–S(10)–C(9)	97.5(6)	Ni–N(16)–C(17)	110.1(9)	S(13)–C(12)–C(11)	115.7(17)
C(18)–S(1)–C(2)–C(3)	−62.1(15)	C(12)–S(13)–C(14)–C(15)	137.8(12)	S(1)–C(2)–C(3)–S(4)	−49.3(18)		
C(2)–S(1)–C(18)–C(17)	134.4(10)	C(12)–C(13)–C(14)–C(15′)	79.4(13)	S(4)–C(5)–C(6)–N(7)	−54.7(16)		
C(2)–S(1)–C(18)–C(17′)	75.7(11)	C(8)–N(7)–C(6)–C(5)	−177.0(14)	N(7)–C(8)–C(9)–S(10)	50.8(18)		
C(5)–S(4)–C(3)–C(2)	−68.4(15)	C(6)–N(7)–C(8)–C(9)	−174.2(14)	S(10)–C(11)–C(12)–S(13)	−45.3(22)		
C(3)–S(4)–C(5)–C(6)	128.9(13)	C(17)–N(16)–C(15)–C(14)	−121.1(17)	S(13)–C(14)–C(15)–N(16)	−57.7(13)		
C(11)–S(10)–C(9)–C(8)	79.9(14)	C(17′)–N(16)–C(15′)–C(14)	123.6(19)	S(13)–C(14)–C(15′)–N(16)	57.7(13)		
C(9)–S(10)–C(11)–C(12)	−70.6(18)	C(15)–N(16)–C(17)–C(18)	−128.0(16)	N(16)–C(17)–C(18)–S(1)	−58.2(12)		
C(14)–S(13)–C(12)–C(11)	−65.3(18)	C(15′)–N(16)–C(17′)–C(18)	115.9(19)	N(16)–C(17′)–C(18)–S(1)	58.3(12)		

ionic radii of Ni^{2+} and S^{2-}, 2.44 Å), 2.376(1)–2.397(1) Å. A similar compression is observed in $[Ni([9]aneS_3)_2]^{2+}$, in which each ligand binds facially to Ni^{II}, Ni–S 2.377(1)–2.400(1) Å.[6] Interestingly however, Ni^{II} co-ordinates to $[24]aneS_6$ (1,5,9,13,17,21-hexathiacyclotetracosane) to give the *rac* isomer, with uncompressed Ni–S bond lengths between 2.415(1) and 2.445(1) Å,[7] very similar to those observed for $[Ni([18]aneN_2S_4)]^{2+}$. The *rac* configuration in $[Ni([24]aneS_6]^{2+}$ results in only eight of the twelve C–S bonds adopting *gauche* placements.

While $[Ni([18]aneS_6)]^{2+}$ is centrosymmetric,[6] $[Ni([18]aneN_2S_4)]^{2+}$, like all other hexadentate complexes of $[18]aneN_2S_4$, shows a tetrahedral distortion of the S-donors out of the least-squares S_4 co-ordination plane. Atoms S(1) and S(13) lie 0.227 and 0.225 Å respectively above the plane, while S(4) and S(10) lie −0.224 and −0.228 Å respectively below.[2]

We were unable to obtain crystals of $[Ni(Me_2[18]aneN_2S_4)][PF_6]_2$ of suitable quality for a structure determination.* However, by analogy with $[Cu(Me_2[18]aneN_2S_4)]^{2+}$ and $[Ag(Me_2[18]aneN_2S_4)]^{+}$, which are the only structurally characterised six-co-ordinate complexes of $Me_2[18]aneN_2S_4$, $[Ni(Me_2[18]aneN_2S_4)]^{2+}$ is most likely to exist as a *meso* isomer **A** involving *facial* binding of the $SCH_2CH_2N(Me)CH_2CH_2S$ linkages.[8,9]

Cyclic voltammetry of $[Ni([18]aneN_2S_4)][PF_6]_2$ in MeCN (0.1 mol dm^{-3} $NBu^n{}_4PF_6$ supporting electrolyte) shows two reversible to quasi-reversible one electron redox processes at $E_{\frac{1}{2}} = +0.98$ (ΔE_p = 75 mV at a scan rate of 100 mV s^{-1}) and −1.51 V (ΔE_p = 120 mV) *vs.* ferrocene–ferrocenium assigned to Ni^{II}–Ni^{III} and Ni^{II}–Ni^{I} couples respectively. Loss of reversibility is observed as the scan rate is decreased. The ESR spectrum (77 K, MeCN glass) of the species obtained by controlled-potential oxidation of $[Ni([18]aneN_2S_4)]^{2+}$ shows

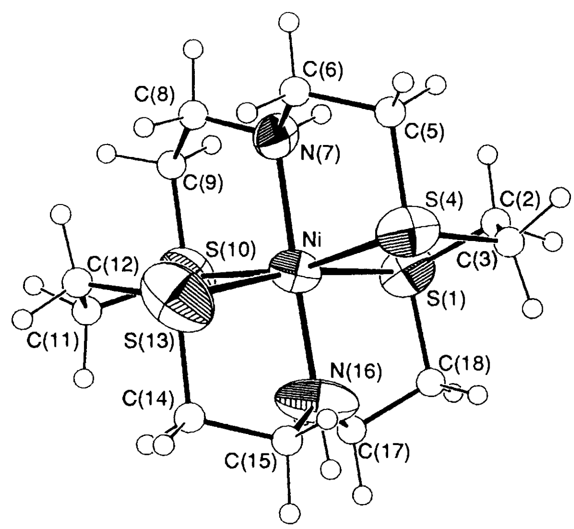

Fig. 1 View of the structure of $[Ni([18]aneN_2S_4)]^{2+}$ with the numbering scheme adopted

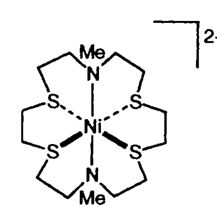

A

a strong rhombic signal with $g_1 = 2.129$, $g_2 = 2.104$ and $g_3 = 2.027$. However, coulometric measurements gave values of greater than one electron (typically 1.3) for this oxidation process suggesting limited decomposition of the nickel(III) product. Comparison of these data with the electrochemical data for $[Ni(Me_2[18]aneN_2S_4)]^{2+}$ below strongly suggests that the redox processes observed are genuinely metal-based. Thus, the oxidation product is assigned as the nickel(III) complex

* A single-crystal structural determination on $[Ni(Me_2[18]aneN_2S_4)][PF_6]_2$ shows that this complex crystallises in the trigonal space group $P\bar{3}m1$ with a = 10.408(12), c = 6.777(5) Å, U = 635.8 Å^3 (by least-squares refinement on diffraction angles for eight centred reflections measured at $\pm\omega$ (λ = 0.710 73 Å), Z = 1, D_c = 1.83 g cm^{-3}. These cell parameters are very similar to those for the *meso* copper(II) analogue[8] and suggest that the nickel(II) complex also shows a *meso* configuration. The nickel position was located from a Patterson synthesis, however the development of the structure was hampered by disorder of the macrocyclic N and S atoms.

$[Ni([18]aneN_2S_4)]^{3+}$. No stable nickel(I) species could be electrogenerated at room temperature.

Cyclic voltammetric measurements on $[Ni(Me_2[18]aneN_2S_4)][PF_6]_2$ under similar conditions show a reversible one-electron reduction at $E_{\frac{1}{2}} = -1.16$ V ($\Delta E_p = 70$ mV at a scan rate of 100 mV s^{-1}), assigned to a Ni^{II}–Ni^{I} couple. Coulometric measurements confirm the reduction to be a one-electron process. The reduction potential for $[Ni(Me_2[18]aneN_2S_4)]^{2+/+}$ is considerably more anodic than that for $[Ni([18]aneN_2S_4)]^{2+/+}$, strongly suggesting a greater interaction of the metal ion with the soft thioether S-donors and less interaction with the N-donors in $[Ni(Me_2[18]aneN_2S_4)]^{2+}$ compared to $[Ni([18]aneN_2S_4)]^{2+}$. We have previously observed this trend in M–S and M–N bond lengths for *meso*-$[Cu(Me_2[18]aneN_2S_4)]^{2+}$ [Cu–S 2.496(5), Cu–N 2.191(17) Å] compared to *rac*-$[Cu([18]aneN_2S_4)]^{2+}$ [Cu–S 2.487(5), 2.528(5), 2.577(5), 2.578(5), Cu–N 2.007(13), 2.036(12) Å].[8] Consistent with this, an irreversible Ni^{II}–Ni^{III} couple is also observed for $[Ni(Me_2[18]aneN_2S_4)]^{2+}$ at a highly anodic potential, $E_{pa} = +1.51$ V. An irreversible reduction at $E_{pc} = -2.17$ V is tentatively assigned to a Ni^{I}–Ni^{0} couple. These data are consistent with our assignment of $[Ni(Me_2[18]aneN_2S_4)]^{2+}$ as a *meso* isomer.

Reaction of $Co(NO_3)_2 \cdot 6H_2O$ with 1 molar equivalent of $[18]aneN_2S_4$ in refluxing aqueous EtOH affords a purple solution. Addition of an excess of NH_4PF_6 and recrystallisation from acetone gives a purple precipitate. The FAB mass spectrum of the complex shows peaks at *m/z* 530 and 384, corresponding to $[^{59}Co([18]aneN_2S_4)(PF_6)]^+$ and $[^{59}Co([18]aneN_2S_4 - H)]^+$ respectively. This evidence, together with IR spectroscopic [ν(N–H) 3260 and 3160 cm^{-1}] and microanalytical data, confirms the formulation $[Co([18]aneN_2S_4)][PF_6]_2$.

Cyclic voltammetry of $[Co([18]aneN_2S_4)][PF_6]_2$ in MeCN solution (0.1 mol dm^{-3} $NBu^n{}_4PF_6$ supporting electrolyte) shows (Fig. 2) two chemically reversible redox couples at $E_{\frac{1}{2}} = -0.07$ ($\Delta E_p = 100$ mV at a scan rate of 230 mV s^{-1}) and -1.30 ($\Delta E_p = 75$ mV). Coulometric measurements in MeCN solution at a platinum-basket electrode confirm that each process corresponds to a one-electron transfer, the first generating an orange solution, while the second gives a light green solution. These processes are assigned to Co^{II}–Co^{III} and Co^{II}–Co^{I} redox couples respectively. The larger peak separation for the former suggests that a significant stereochemical change occurs at the metal centre upon oxidation. This may reflect the inertness of the low-spin d^6 cobalt(III) centre and high Co–S bond strength. In contrast, cleavage of M–S and/or M–N to give a square-planar cobalt(I) species is rapid relative to the rate of electron transfer. The oxidation potential for $[Co([18]aneN_2S_4)]^{2+}$ is only slightly less anodic than that for $[Co([18]aneS_6)]^{2+/3+}$, while the reduction potential is more cathodic.[10] This reflects the incorporation of two N donor atoms which have no π-bonding capacity. Also, the reversibility of the Co^{II}–Co^{I} redox couple for $[Co([18]aneN_2S_4)]^{2+}$ contrasts with the irreversibility of that for $[Co([18]aneS_6)]^{2+}$. The Co^{II}–Co^{III} couple for $[Co([18]aneN_6)]^{3+}$ ($[18]aneN_6$ = 1,4,7,10,13,16-hexaazacyclooctadecane) occurs at -1.13 V *vs.* ferrocene–ferrocenium,[11] while for $[Co([9]aneN_3)_2]^{3+}$ ($[9]aneN_3$ = 1,4,7-triazacyclononane) it is slightly less cathodic, at $E_{\frac{1}{2}} = -0.87$ V.[12]

Aerial oxidation of the $[Co([18]aneN_2S_4)]^{2+}$ cation occurs in aqueous solution over a few days, yielding dark orange crystals of the corresponding low-spin d^6 cobalt(III) complex $[Co([18]aneN_2S_4)][PF_6]_3 \cdot 3H_2O$. In our previous work we have shown that the cations $[M([18]aneN_2S_4)]^{x+}$ (M = Fe, Cu or Hg, $x = 2$; M = Rh, $x = 3$; M = Ag, $x = 1$) adopt the *rac* configuration involving *meridional* binding of the two $SCH_2CH_2N(H)CH_2CH_2S$ linkages of the crown to the metal ion.[2,8,9,13–15] In order to determine whether this is also true for Co^{III}, and to evaluate the extent of the tetrahedral distortion of the four S donors around the smaller Co^{III}, we undertook a single-crystal X-ray analysis on $[Co([18]aneN_2S_4)][PF_6]_3 \cdot 3H_2O$. The structure shows (Fig. 3, Table 2) the Co^{III} encapsulated by the hexadentate crown ether giving an overall distorted octahedral geometry, Co–S 2.268(1), 2.249(1), 2.252(1), 2.254(1), Co–N 1.993(4), 1.994(4) Å, and confirms a *rac* configuration similar to that observed for other first-row metal complexes with this compound. In this case, the tetrahedral distortion from the best S_4 co-ordination plane is smaller, with S(1) and S(10) lying above this plane by 0.120 Å, while S(4) and S(13) lie 0.120 Å below. The extent of this distortion is considerably less than that observed for $[Ni([18]aneN_2S_4)]^{2+}$, and clearly reflects the smaller ionic radius for Co^{III} compared to Ni^{II}. Extensive hydrogen bonding is also evident from the structure determination (Fig. 4, Table 3), involving the three H_2O solvent molecules which are associated per cation, the NH functions of the $[Co([18]aneN_2S_4)]^{3+}$ cation and the $PF_6{}^-$ anions.

Electronic Spectroscopy.—The electronic spectrum of $[Ni([18]aneN_2S_4)]^{2+}$ shows, in addition to two charge-transfer transitions at $\lambda_{max} = 303$ (ε = 9200) and 262 (3350), two much weaker d–d transitions at 824 (ε = 21) and 546 nm (68 dm^3 mol^{-1} cm^{-1}). The related complex $[Ni(Me_2[18]aneN_2S_4)]^{2+}$ also shows two charge-transfer transitions at $\lambda_{max} = 312$ (ε = 5230) and 273 (2960), as well as two d–d bands at 903 (59) and 574 nm (53 dm^3 mol^{-1} cm^{-1}). These spectra are indicative of approximate octahedral local symmetry at Ni^{II}. Under these

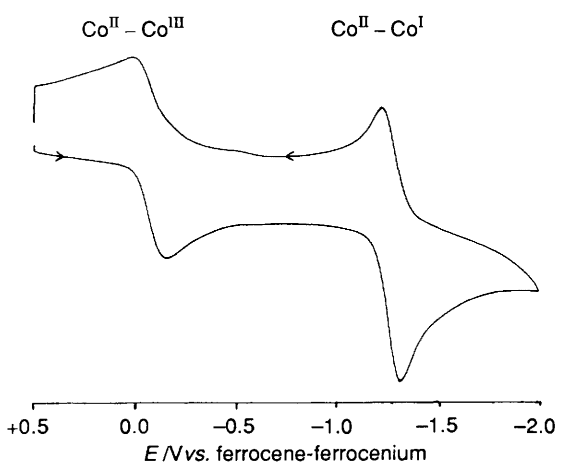

Fig. 2 Cyclic voltammogram for $[Co([18]aneN_2S_4)][PF_6]_2$ (MeCN, 0.1 mol dm^{-3} $NBu^n{}_4PF_6$ supporting electrolyte)

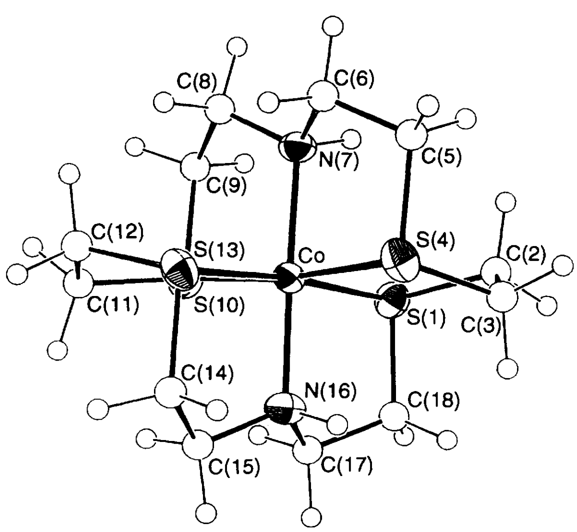

Fig. 3 View of the structure of $[Co([18]aneN_2S_4)]^{3+}$ with the numbering scheme adopted

Table 2 Bond lengths (Å), angles and torsion angles (°) for $[Co([18]aneN_2S_4)]^{3+}$

Co–S(1)	2.268(1)	S(1)–C(2)	1.817(5)	C(6)–N(7)	1.494(6)	C(12)–S(13)	1.821(5)		
Co–S(4)	2.249(1)	S(1)–C(18)	1.831(5)	N(7)–C(8)	1.494(6)	S(13)–C(14)	1.821(5)		
Co–N(7)	1.993(4)	C(2)–C(3)	1.519(7)	C(8)–C(9)	1.514(7)	C(14)–C(15)	1.496(7)		
Co–S(10)	2.252(1)	C(3)–S(4)	1.810(5)	C(9)–S(10)	1.830(5)	C(15)–N(16)	1.490(6)		
Co–S(13)	2.254(1)	S(4)–C(5)	1.828(5)	S(10)–C(11)	1.811(5)	N(16)–C(17)	1.493(6)		
Co–N(16)	1.994(4)	C(5)–C(6)	1.504(7)	C(11)–C(12)	1.499(7)	C(17)–C(18)	1.495(7)		

S(1)–Co–S(4)	90.43(5)	S(10)–Co–S(13)	90.45(5)	S(4)–C(5)–C(6)	108.7(4)	Co–S(13)–C(12)	105.1(2)
S(1)–Co–N(7)	93.17(12)	S(10)–Co–N(16)	94.67(11)	C(5)–C(6)–N(7)	108.5(4)	Co–S(13)–C(14)	97.58(16)
S(1)–Co–S(10)	89.29(5)	S(13)–Co–N(16)	87.68(11)	Co–N(7)–C(6)	112.2(3)	C(12)–S(13)–C(14)	104.0(2)
S(1)–Co–S(13)	173.9(1)	Co–S(1)–C(2)	103.6(2)	Co–N(7)–C(8)	114.5(3)	S(13)–C(14)–C(15)	111.0(3)
S(1)–Co–N(16)	86.21(11)	Co–S(1)–C(18)	98.67(16)	C(6)–N(7)–C(8)	111.1(4)	C(14)–C(15)–N(16)	109.0(4)
S(4)–Co–N(7)	86.26(12)	C(2)–S(1)–C(18)	102.2(2)	N(7)–C(8)–C(9)	108.3(4)	Co–N(16)–C(15)	114.7(3)
S(4)–Co–S(10)	173.9(1)	S(1)–C(2)–C(3)	112.1(3)	C(8)–C(9)–S(10)	111.0(4)	Co–N(16)–C(17)	111.9(3)
S(4)–Co–S(13)	90.48(5)	C(2)–C(3)–S(4)	112.9(3)	Co–S(10)–C(9)	98.13(17)	C(15)–N(16)–C(17)	112.4(3)
S(4)–Co–N(16)	91.41(11)	Co–S(4)–C(3)	103.9(2)	Co–S(10)–C(11)	104.5(2)	N(16)–C(17)–C(18)	108.2(4)
N(7)–Co–S(10)	87.65(12)	Co–S(4)–C(5)	99.65(17)	C(9)–S(10)–C(11)	104.4(2)	S(1)–C(18)–C(17)	109.6(3)
N(7)–Co–S(13)	92.96(12)	C(3)–S(4)–C(5)	102.4(2)	S(10)–C(11)–C(12)	114.9(3)		
N(7)–Co–N(16)	177.6(2)			C(11)–C(12)–S(13)	114.3(3)		

C(18)–S(1)–C(2)–C(3)	−67.1(4)	C(5)–C(6)–N(7)–C(8)	−176.2(4)	C(11)–C(12)–S(13)–C(14)	−76.3(4)
C(2)–S(1)–C(18)–C(17)	130.7(3)	C(6)–N(7)–C(8)–C(9)	−174.9(4)	C(12)–S(13)–C(14)–C(15)	76.0(4)
S(1)–C(2)–C(3)–S(4)	−47.7(4)	N(7)–C(8)–C(9)–S(10)	48.2(5)	S(13)–C(14)–C(15)–N(16)	49.3(4)
C(2)–C(3)–S(4)–C(5)	−68.1(4)	C(8)–C(9)–S(10)–C(11)	79.0(4)	C(14)–C(15)–N(16)–C(17)	−173.1(4)
C(3)–S(4)–C(5)–C(6)	131.8(4)	C(9)–S(10)–C(11)–C(12)	−71.9(4)	C(15)–N(16)–C(17)–C(18)	−174.1(4)
S(4)–C(5)–C(6)–N(7)	−50.2(5)	S(10)–C(11)–C(12)–S(13)	−38.1(5)	N(16)–C(17)–C(18)–S(1)	−50.6(4)

Table 3 Hydrogen-bonding parameters (lengths in Å, angles in °) for $[Co([18]aneN_2S_4)][PF_6]_3{\cdot}3H_2O$

H(7)···O(2S)	1.756(6)	H(2SA)···F(16)	2.18(4)	H(16)···O(1S)	1.929(5)	H(2SB)···O(1S)	2.53(5)
H(1SA)···F(26)	2.48(4)	H(3SA)···F(25)	2.30(5)	H(1SB)···F(36)	2.11(4)	H(3SB)···O(2S)	1.92(5)

N(7)–H(7)···O(2S)	162.5(4)	O(1S)–H(1SA)···F(26)	159(4)	H(1SB)–O(1S)···H(2SB)	113(3)
H(2SA)–O(2S)···H(7)	99(3)	O(1S)–H(1SB)···F(36)	165(4)	O(3S)–H(3SA)···F(25)	133(4)
H(2SB)–O(2S)···H(7)	88(3)	O(2S)–H(2SA)···F(16)	133(4)	O(3S)–H(3SB)···O(2S)	142(4)
N(16)–H(16)···O(1S)	158.9(4)	O(2S)–H(2SB)···O(1S)	140(4)	H(2SA)–O(2S)···H(3SB)	89(3)
H(1SA)–O(1S)···H(16)	100(3)	H(1SA)–O(1S)···H(2SB)	116(3)	H(2SB)–O(2S)···H(3SB)	138(3)
H(1SB)–O(1S)···H(16)	112(3)				

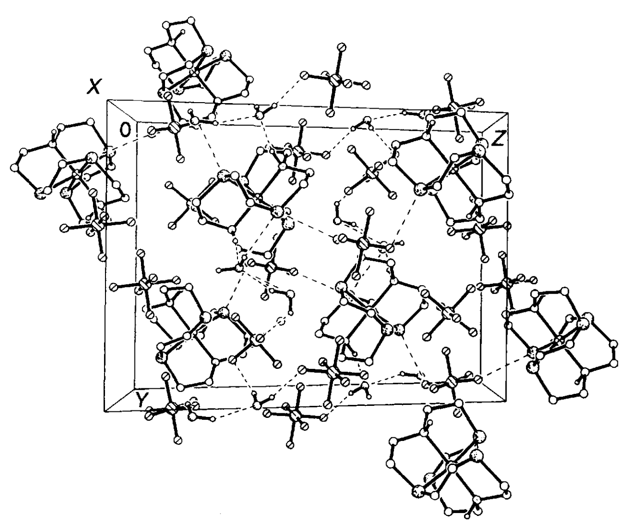

Fig. 4 Packing diagram of $[Co([18]aneN_2S_4)][PF_6]_3{\cdot}3H_2O$ showing the extensive hydrogen-bonding network

conditions three d–d transitions are predicted, the highest-energy absorption ($^3A_2 \longrightarrow {}^3T_1$) being most likely obscured by the charge-transfer bands. The lowest-energy transition corresponds to $^3A_{2g} \longrightarrow {}^3T_{2g} = 10Dq$, and hence allows comparison of ligand-field strengths for a series of nickel(II) complexes involving N- and S-donor macrocyclic ligands (Table 4). As expected, the ligand field exerted on Ni^{II} by $[18]aneN_2S_4$ is intermediate between that of $[18]aneN_6$ and $[18]aneS_6$, but higher than that of $Me_2[18]aneN_2S_4$, reflecting the effect of the secondary amine functions compared to tertiary amines and the different configurations of the two N/S-donor complexes.[19]

The electronic spectrum of $[Co([18]aneN_2S_4)][PF_6]_2$ measured in MeCN solution exhibits two weak transitions at λ_{max} = 593 (ε = 68) and 534 nm (73 dm^3 mol^{-1} cm^{-1}). In addition, two considerably more intense S→Co charge-transfer transitions are apparent at 298 (2390) and 247 nm (4795 dm^3 mol^{-1} cm^{-1}). The weak features are assigned to the $^2E_g \longrightarrow {}^2T_{2g}$ and $^2E_g \longrightarrow {}^2T_{1g}$ d–d transitions, consistent with low-spin Co^{II} in an approximately octahedral field. The generation of such a species with an N_2S_4 donor set reflects the strong ligand field imparted by the thioether donor atoms. The electronic spectra of the related complexes $[Co([9]aneS_3)_2]^{2+}$ and $[Co([9]aneN_3)_2]^{2+}$ are consistent with low- and high-spin Co^{II} respectively,[12] and Sargeson and co-workers[20] have shown that low-spin Co^{II} is also preferred when the metal ion is encapsulated by a N_3S_3-donor cage ligand.

The electronic spectrum of the d^6 cobalt(III) complex $[Co([18]aneN_2S_4)][PF_6]_3$ in aqueous solution also approximates to O_h local symmetry, with the $^1A_{1g} \longrightarrow {}^1T_{1g}$ transition at λ_{max} = 492 nm and the $^1A_{1g} \longrightarrow {}^1T_{2g}$ transition occurring as a shoulder at *ca.* 380 nm. Two much more intense charge-transfer transitions occur at λ_{max} = 326 and 244 nm.

Experimental

Infrared spectra were measured as KBr and CsI discs using a Perkin-Elmer 598 spectrometer over the range 200–4000 cm^{-1}, electronic spectra in quartz cells using a Perkin-Elmer Lambda

Table 4 Selected electronic spectroscopic data for some octahedral N- and S-donor macrocyclic nickel complexes

Complex	λ_{max}/nm (ε/dm^3 mol^{-1} cm^{-1})*	10*Dq*/ cm^{-1}	Ref.
$[Ni([9]aneS_3)_2]^{2+}$	790 (30) 530 (30)	12 755	12
$[Ni([9]aneN_3)_2]^{2+}$	816 (107) 549 (97)	12 500	16
$[Ni([18]aneS_6)]^{2+}$	815 (25) 520 (27)	12 290	7
$[Ni([18]aneN_2S_4)]^{2+}$	824 (21) 546 (68)	12 135	This work
$[Ni([12]aneS_3)_2]^{2+}$	890 (25) 570 (34)	11 240	17
$[Ni([18]aneN_6)]^{2+}$	893 (21) 552 (64)	11 200	18
$[Ni(Me_2[18]aneN_2S_4)]^{2+}$	903 (59) 574 (53)	11 075	This work
$[Ni([24]aneS_6)]^{2+}$	905 (100) 590 (70)	11 050	7

* In each case the bands correspond to the $^3A_{2g} \longrightarrow {}^3T_{2g}$ (low energy) and the $^3A_{2g} \longrightarrow {}^3T_{1g}$ transition (higher energy).

9 spectrophotometer and mass spectra by fast-atom bombardment (FAB) on a Kratos MS 50TC spectrometer. Electrochemical measurements were performed on a Bruker E310 Universal Modular Polarograph. All readings were taken using a three-electrode potentiostatic system in acetonitrile containing 0.1 mol dm^{-3} $NBu^n{}_4PF_6$ or $NBu^n{}_4BF_4$ as supporting electrolyte. Cyclic voltammetric measurements were carried out using a double platinum electrode and a Ag–AgCl reference electrode. All potentials are quoted *versus* ferrocene–ferrocenium.

(*a*) *Synthesis of* $[Ni([18]aneN_2S_4)][PF_6]_2$.—Reaction of $Ni(NO_3)_2 \cdot 6H_2O$ (36 mg, 0.123 mmol) with $[18]aneN_2S_4$ (40 mg, 0.123 mmol) in refluxing EtOH–water (1:1 v/v, 30 cm^3) under N_2 for 1 h yielded a purple solution. After cooling, addition of an excess of NH_4PF_6 afforded a purple precipitate. Recrystallisation from aqueous solution gave a purple crystalline material. Yield: 85% (Found: C, 20.7; H, 3.85; N, 4.30; S, 18.8. $C_{12}H_{26}F_{12}N_2NiP_2S_4$ requires C, 21.3; H, 3.90; N, 4.15; S, 19.0%). FAB mass spectrum (3-nitrobenzyl alcohol matrix): found *m/z* 529 and 383; calc. 529 for $[^{58}Ni([18]aneN_2S_4)(PF_6)]^+$ and 384 for $[^{58}Ni([18]aneN_2S_4)]^+$. Electronic spectrum (MeCN solution): λ_{max} = 824 (ε = 21), 546 (68), 303 (9200) and 262 nm (3350 dm^3 mol^{-1} cm^{-1}). IR spectrum (KBr disc): 3280m, 3180w, 2920m, 2880w, 1555m, 1470m, 1430m, 1420m, 1380w, 1320m, 1290w, 1265w, 1240w, 1210w, 1150w, 1135w, 1090m, 1050w, 1020m, 1000w, 970m, 840vs, 790w, 740m, 640w, 555vs and 460w cm^{-1}.

(*b*) *Structure Determination of* $[Ni([18]aneN_2S_4)][PF_6]_2 \cdot 0.33H_2O$.—Purple crystals of the complex were obtained by slow evaporation from a solution of the complex in MeCN–EtOH (1:1 v/v). The selected crystal (0.20 × 0.20 × 0.40 mm) was sealed in a glass capillary tube to prevent solvent loss.

Crystal data. $C_{12}H_{26}F_{12}N_2NiP_2S_4 \cdot 0.33H_2O$, *M* = 681.2, orthorhombic, space group *Pcab*, *a* = 12.8260(20), *b* = 18.083(3), *c* = 22.200(4) Å, *U* = 5148.8 Å^3 [from 2θ values of 52 reflections measured at ±ω (2θ = 10–21°, λ = 0.710 73 Å)], *Z* = 8, D_c = 1.76 g cm^{-3}, *T* = 298 K, μ = 1.754 mm^{-1}, *F*(000) = 3280.

Data collection and processing. Stoe STADI-4 four-circle diffractometer, graphite-monochromated Mo-Kα X-radiation, *T* = 298 K, ω–2θ scans using the learnt-profile method,[21] 3671 data collected ($2\theta_{max}$ 45°, *h* 0–12, *k* 0–19, *l* 0–23) [3182 unique (R_{int} = 0.0479)] giving 1454 reflections with $F > 4\sigma(F)$ for use in all calculations. No significant crystal decay or movement was observed and no absorption correction was applied.

Structure solution and refinement. The Ni atom was located by a Patterson synthesis and iterative cycles of least-squares refinement and Fourier-difference syntheses located all non-H atoms.[22] During refinement the presence of both diastereoisomeric forms of the *rac* isomer became evident and was modelled by refining the C–C–N units as rigid groups with bond lengths of 1.50 Å and tetrahedral angles around each of these atoms. This successfully defined two alternative sites for each C adjacent to N as a 50:50 mixture. One of the PF_6^- anions also showed severe disorder, which was modelled reasonably well by using partial F atom occupancies, with the constraint that the total number of F atoms per P atom summed to six. One partially occupied H_2O solvent molecule was found per cation. Hydrogen atoms were included in fixed, calculated positions. Anisotropic thermal parameters were refined for Ni, S, P, N, all fully occupied C atoms and all F atoms with occupancies greater than 50%. The weighting scheme $w^{-1} = \sigma^2(F) + 0.002\,17F^2$ gave satisfactory agreement analyses. At final convergence *R*, *R'* = 0.0794, 0.0976 respectively, *S* = 1.167 for 285 refined parameters and the final Δ*F* synthesis showed no peak above 0.98 or below −0.58 e Å^{-3}. Atomic scattering factors were inlaid,[22] or taken from ref. 23. Molecular geometry calculations utilised CALC[24] and the Figures were produced by ORTEP II.[25] Selected bond lengths, angles and torsion angles are given in Table 1, fractional atomic coordinates in Table 5.

(*c*) *Synthesis of* $[Ni(Me_2[18]aneN_2S_4)][PF_6]_2$.—As in (*a*) above, using $Ni(NO_3)_2 \cdot 6H_2O$ (36 mg, 0.123 mmol) and $Me_2[18]aneN_2S_4$ (40 mg, 0.123 mmol). The product was isolated as a blue microcrystalline solid. Yield: 70% (Found: C, 24.3; H, 4.25; N, 4.15; S, 18.2. $C_{14}H_{30}F_{12}N_2NiP_2S_4$ requires C, 23.9; H, 4.30; N, 4.00; S, 18.3%). FAB mass spectrum: found *m/z* 557, 431 and 412; calc. 557 for $[^{58}Ni(Me_2[18]aneN_2S_4)(PF_6)]^+$, 430 for $[^{58}Ni(Me_2[18]aneN_2S_4)(H_2O)]^+$ and 412 for $[^{58}Ni(Me_2[18]aneN_2S_4)]^+$. Electronic spectrum (MeCN solution): λ_{max} = 903 (ε = 59), 574 (53), 312 (5230) and 273 nm (2960 dm^3 mol^{-1} cm^{-1}). IR spectrum (KBr disc): 3010w, 2940w, 1470m, 1430m, 1380w, 1320m, 1270w, 1230w, 1210w, 1160w, 1140w, 1070w, 1030w, 1005w, 990m, 840vs, 745m, 685w, 640w, 620w, 555vs and 460w cm^{-1}.

(*d*) *Synthesis of* $[Co([18]aneN_2S_4)][PF_6]_2$.—As in (*a*), using $Co(NO_3)_2 \cdot 6H_2O$ (36 mg, 0.123 mmol) and $[18]aneN_2S_4$ (40 mg, 0.123 mmol). Recrystallisation from aqueous solution gave a deep purple crystalline material. Yield: 73% (Found: C, 20.8; H, 3.90; N, 4.15; S, 19.4. $C_{12}H_{26}CoF_{12}N_2P_2S_4$ requires C, 21.3; H, 3.85; N, 4.15; S, 19.0%). FAB mass spectrum: found *m/z* 530 and 384; calc. 530 for $[^{59}Co([18]aneN_2S_4)(PF_6)]^+$ and 384 for $[^{59}Co([18]aneN_2S_4 - H)]^+$. Electronic spectrum (MeCN solution): λ_{max} = 593 (ε = 68), 534 (73), 298 (2390) and 247 nm (4795 dm^3 mol^{-1} cm^{-1}). IR spectrum (KBr disc): 3260m, 3160m, 2920w, 2880w, 1470m, 1415m, 1385w, 1320w, 1300w, 1285w, 1260w, 1240w, 1210w, 1145w, 1100w, 1070w, 1025w, 1010m, 980w, 840vs, 790m, 640w and 555vs cm^{-1}.

(*e*) *Structure Determination of* $[Co([18]aneN_2S_4)][PF_6]_3 \cdot 3H_2O$.—Slow recrystallisation of $[Co([18]aneN_2S_4)][PF_6]_2$ from aqueous solution resulted in aerial oxidation generating $[Co([18]aneN_2S_4)][PF_6]_3 \cdot 3H_2O$ as dark red crystals. A single red tablet (0.70 × 0.45 × 0.25 mm) was selected for a crystallographic study.

Crystal data. $C_{12}H_{26}CoF_{18}N_2P_3S_4 \cdot 3H_2O$, *M* = 874.45, monoclinic, space group $P2_1/n$, *a* = 11.5485(3), *b* = 13.9779(2), *c* = 19.1378(4) Å, β = 106.561(2)°, *U* = 2961 Å^3 [from 2θ values of 38 reflections measured at ±ω (2θ = 30–32°, λ = 0.710 73 Å)], *Z* = 4, D_c = 1.96 g cm^{-3}, *T* = 298 K, μ = 1.084 mm^{-1}, *F*(000) = 1760.

Data collection and processing. As in (*b*) except as stated: ω–2θ scans with ω-scan width (1.05 + 0.347 tan θ)°, 3739 unique data

Table 5 Fractional atomic coordinates for $[Ni([18]aneN_2S_4)][PF_6]_2 \cdot 0.33H_2O$

Atom	*x*	*y*	*z*	Atom	*x*	*y*	*z*
Ni	0.224 04(15)	0.098 02(11)	0.128 65(10)	F(12)	0.528 1(9)	0.205 9(9)	0.445 5(6)
S(1)	0.344 8(3)	0.155 0(3)	0.197 45(24)	F(13)	0.551 5(23)	0.323 3(14)	0.395 9(13)
S(4)	0.099 8(3)	0.092 3(3)	0.211 17(24)	F(14)	0.386(3)	0.272 9(25)	0.419 2(17)
S(10)	0.329 0(4)	0.127 6(3)	0.042 3(3)	F(15)	0.592 6(21)	0.225 9(14)	0.353 5(13)
S(13)	0.119 3(4)	0.022 1(4)	0.062 7(3)	F(16)	0.451 0(25)	0.168 7(16)	0.372 9(15)
N(7)	0.146 3(9)	0.198 8(7)	0.108 3(6)	C(2)	0.262 0(14)	0.176 1(11)	0.260 2(9)
N(16)	0.297 7(9)	0.000 2(7)	0.150 8(7)	C(3)	0.181 2(13)	0.123 0(10)	0.275 0(8)
P(1)	0.220 3(5)	0.402 8(3)	0.153 9(4)	C(5)	0.028 3(13)	0.176 1(10)	0.193 6(8)
F(1)	0.166 9(14)	0.475 5(9)	0.136 8(8)	C(6)	0.035 3(12)	0.194 5(11)	0.127 6(8)
F(2)	0.184 5(13)	0.420 1(12)	0.216 4(7)	C(8)	0.155 1(14)	0.219 7(11)	0.047 5(9)
F(3)	0.245 7(17)	0.389 6(8)	0.087 8(9)	C(9)	0.268 2(13)	0.217 0(10)	0.024 5(8)
F(4)	0.320 9(9)	0.447 1(7)	0.159 1(8)	C(11)	0.277 3(16)	0.066 2(13)	−0.017 5(10)
F(5)	0.276 0(10)	0.326 0(7)	0.159 6(10)	C(12)	0.163 9(16)	0.047 8(14)	−0.012 2(11)
F(6)	0.114 5(10)	0.358 1(8)	0.144 9(9)	C(14)	0.188 4(12)	−0.064 6(5)	0.077 3(7)
P(2)	0.493 2(4)	0.247 0(4)	0.387 52(23)	C(15)	0.228 1(12)	−0.065 3(7)	0.140 8(8)
F(7)	0.508 2(24)	0.188(3)	0.341 1(18)	C(15′)	0.298 4(9)	−0.048 4(10)	0.096 1(6)
F(8)	0.482 5(22)	0.308 7(16)	0.431 1(12)	C(17)	0.408 3(8)	0.015 1(4)	0.169 2(8)
F(9)	0.382 7(14)	0.223 3(18)	0.395 4(12)	C(17′)	0.335 6(15)	0.005 6(3)	0.214 6(6)
F(10)	0.456 2(10)	0.288 2(9)	0.330 0(6)	C(18)	0.409 8(10)	0.069 4(4)	0.220 3(6)
F(11)	0.615 3(15)	0.257 8(20)	0.381 7(10)	O(1S)	0.471(3)	−0.039 4(23)	0.060 4(19)

Table 6 Fractional atomic coordinates for $[Co([18]aneN_2S_4)][PF_6]_3 \cdot 3H_2O$

Atom	*x*	*y*	*z*	Atom	*x*	*y*	*z*
Co	0.082 57(5)	0.202 47(4)	0.848 81(3)	F(13)	0.312 4(3)	0.026 6(3)	0.176 14(17)
S(1)	0.273 24(10)	0.151 12(8)	0.903 18(6)	F(14)	0.389 7(3)	−0.068 38(21)	0.106 43(21)
C(2)	0.353 7(4)	0.179 5(3)	0.837 0(3)	F(15)	0.473 5(3)	0.060 6(3)	0.069 73(20)
C(3)	0.308 8(4)	0.271 6(3)	0.796 1(3)	F(16)	0.512 77(25)	0.027 67(22)	0.189 66(17)
S(4)	0.145 83(10)	0.277 13(8)	0.762 26(6)	P(2)	0.528 65(13)	0.196 10(9)	0.654 07(7)
C(5)	0.112 2(5)	0.184 4(4)	0.691 97(25)	F(21)	0.663 8(4)	0.177 7(5)	0.667 8(3)
C(6)	0.012 6(5)	0.122 0(4)	0.702 7(3)	F(22)	0.503 6(4)	0.110 9(3)	0.596 75(25)
N(7)	0.045 1(3)	0.091 5(3)	0.780 69(20)	F(23)	0.522 3(6)	0.263 6(3)	0.588 86(24)
C(8)	−0.046 7(5)	0.023 9(4)	0.793 8(3)	F(24)	0.553 5(5)	0.278 9(3)	0.710 1(3)
C(9)	−0.014 6(5)	0.003 1(3)	0.874 6(3)	F(25)	0.389 2(4)	0.208 7(5)	0.640 7(3)
S(10)	0.016 63(10)	0.113 66(8)	0.927 95(6)	F(26)	0.526 4(7)	0.128 0(4)	0.716 4(3)
C(11)	−0.131 2(4)	0.161 8(4)	0.922 3(3)	P(3)	0.129 04(11)	0.102 31(9)	0.450 06(7)
C(12)	−0.197 9(4)	0.202 3(4)	0.849 5(3)	F(31)	−0.010 6(3)	0.078 79(25)	0.420 72(20)
S(13)	−0.102 99(10)	0.266 19(9)	0.803 75(6)	F(32)	0.266 6(3)	0.130 1(4)	0.476 48(21)
C(14)	−0.073 4(4)	0.380 3(3)	0.851 4(3)	F(33)	0.141 1(4)	0.090 3(3)	0.370 28(19)
C(15)	0.018 3(4)	0.369 4(3)	0.924 0(3)	F(34)	0.152 8(4)	−0.007 0(3)	0.463 7(3)
N(16)	0.124 2(3)	0.315 81(24)	0.914 45(18)	F(35)	0.098 7(4)	0.212 39(25)	0.434 9(3)
C(17)	0.213 7(4)	0.291 6(3)	0.985 49(25)	F(36)	0.117 6(4)	0.113 8(3)	0.529 34(20)
C(18)	0.321 6(4)	0.247 5(4)	0.969 95(25)	O(1S)	0.282 7(4)	−0.014 0(3)	0.644 48(23)
P(1)	0.393 60(11)	0.043 28(9)	0.123 22(7)	O(2S)	0.233 2(4)	−0.042 6(3)	0.806 2(3)
F(11)	0.398 4(3)	0.154 74(21)	0.139 55(18)	O(3S)	0.723 0(6)	0.132 8(5)	0.061 9(4)
F(12)	0.273 69(25)	0.058 38(22)	0.057 58(16)				

measured, ($2\theta_{max}$ 45°, *h* −12 to 11, *k* 0–15, *l* 0–20) giving 3297 reflections with $F > 6\sigma(F)$ for use in all calculations.

Structure solution and refinement. As in (*b*) except as stated: the Co atom was located in a Patterson synthesis. The cation and three PF_6^- anions were well ordered. During refinement three fully occupied H_2O solvent molecules were found to be hydrogen-bonded to each cation: these were refined with the O–H bond lengths restrained to be 0.96 Å and the H–O–H angle to be tetrahedral. Non-H atoms were then refined (by least squares on *F*)[22] with anisotropic thermal parameters, and the H atoms were included at fixed, calculated positions. At final convergence, $R, R' = 0.0397, 0.0549$ respectively, $S = 1.234$ for 406 refined parameters and the final ΔF synthesis showed no peak above 0.73 or below −0.37 e Å^{-3}. The weighting scheme $w^{-1} = \sigma^2(F) + 0.000\,257F^2$ gave satisfactory agreement analyses. Selected bond lengths, angles and torsion angles are given in Table 2, fractional atomic coordinates in Table 6.

Additional material available for both structures from the Cambridge Crystallographic Data Centre comprises H-atom coordinates, thermal parameters and remaining bond lengths and angles.

Acknowledgements

We thank the SERC for support.

References

1 P. Chaudhuri and K. Wieghardt, *Prog. Inorg. Chem.*, 1987, **35**, 329; A. J. Blake and M. Schröder, *Adv. Inorg. Chem.*, 1990, **35**, 1; S. R. Cooper and S. C. Rawle, *Struct. Bonding (Berlin)*, 1990, **72**, 1; P. V. Bernhardt and G. A. Lawrence, *Coord. Chem. Rev.*, 1990, **104**, 297.

2 G. Reid and M. Schröder, *Chem. Soc. Rev.*, 1990, **19**, 239.

3 A. J. Blake, R. O. Gould, A. J. Holder, T. I. Hyde and M. Schröder, *J. Chem. Soc., Dalton Trans.*, 1988, 1861; S. C. Rawle, R. Yagbasan and S. R. Cooper, *J. Am. Chem. Soc.*, 1987, **109**, 6181; D. Collison, G. Reid and M. Schröder, *Polyhedron*, 1992, **11**, 3165; A. J. Blake, R. O. Gould, J. A. Greig, A. J. Holder, T. I. Hyde and M. Schröder, *J. Chem. Soc., Chem. Commun.*, 1989, 876; A. J. Blake, J. A. Greig, A. J. Holder, T. I. Hyde, A. Taylor and M. Schröder, *Angew. Chem.*, 1990, **102**, 203; *Angew. Chem., Int. Ed. Engl.*, 1990, **29**, 197; A. J. Blake, A. Taylor and M. Schröder, *J. Chem. Soc., Chem. Commun.*, 1993, 1097; A. J. Blake, R. O. Gould, G. Reid and M. Schröder, *J. Chem. Soc., Chem. Commun.*, 1990, 974; A. J. Blake, R. O. Gould, T. I. Hyde and M. Schröder, *J. Chem. Soc., Chem. Commun.*, 1987, 431;

A. J. Blake, L. M. Gordon, A. J. Holder, T. I. Hyde, G. Reid and M. Schröder, *J. Chem. Soc., Chem. Commun.*, 1988, 1452; A. J. Blake, D. Collison, R. O. Gould, G. Reid and M. Schröder, *J. Chem. Soc., Dalton Trans.*, 1993, 521.
4 G. Reid, A. J. Blake, T. I. Hyde and M. Schröder, *J. Chem. Soc., Chem. Commun.*, 1988, 1397; A. J. Blake, G. Reid and M. Schröder, *J. Chem. Soc., Dalton Trans.*, 1990, 3363.
5 A. J. Blake, A. J. Holder, T. I. Hyde and M. Schröder, *J. Chem. Soc., Chem. Commun.*, 1987, 987; A. J. Blake, A. J. Holder, T. I. Hyde, A. J. Lavery, Y. V. Roberts and M. Schröder, *J. Organomet. Chem.*, 1987, **323**, 261.
6 S. R. Cooper, S. C. Rawle, J. A. R. Hartman, E. J. Hintsa and G. A. Adams, *Inorg. Chem.*, 1988, **27**, 1209.
7 S. C. Rawle, J. A. R. Hartman, D. J. Watkin and S. R. Cooper, *J. Chem. Soc., Chem. Commun.*, 1986, 1083.
8 N. Atkinson, A. J. Blake, M. G. B. Drew, G. Forsyth, A. J. Lavery, G. Reid and M. Schröder, *J. Chem. Soc., Chem. Commun.*, 1989, 984; N. Atkinson, A. J. Blake, M. G. B. Drew, G. Forsyth, R. O. Gould, A. J. Lavery, G. Reid and M. Schröder, *J. Chem. Soc., Dalton Trans.*, 1992, 2993; see also P. D. Beer, J. E. Nation, S. L. W. McWhinnie, M. E. Harman, M. B. Hursthouse, M. I. Ogden and A. H. White, *J. Chem. Soc., Dalton Trans.*, 1991, 2485.
9 A. J. Blake, G. Reid and M. Schröder, *J. Chem. Soc., Dalton Trans.*, 1991, 615.
10 J. A. R. Hartman, E. J. Hintsa and S. R. Cooper, *J. Am. Chem. Soc.*, 1986, **108**, 1208.
11 R. W. Hay, B. Jeragh, S. F. Lincoln and G. H. Searle, *Inorg. Nucl. Chem. Lett.*, 1978, **14**, 435.
12 K. Wieghardt, H. J. Küppers and J. Weiss, *Inorg. Chem.*, 1985, **24**, 3067.
13 N. Atkinson, A. J. Blake, A. J. Lavery, G. Reid and M. Schröder, *Polyhedron*, 1990, **9**, 2641.
14 A. J. Blake, G. Reid and M. Schröder, *Polyhedron*, 1990, **9**, 2931.
15 A. J. Blake, G. Reid and M. Schröder, *Polyhedron*, 1990, **9**, 2925.
16 R. Yang and L. Zompa, *Inorg. Chem.*, 1976, **15**, 1499.
17 S. R. Cooper, S. C. Rawle, J. A. R. Hartman, E. J. Hintsa and G. A. Adams, *Inorg. Chem.*, 1988, **27**, 1209.
18 A. Bencine, L. Fabbrizzi and A. Poggi, *Inorg. Chem.*, 1981, **20**, 2544.
19 N. Sutin and P. Gutlich, *Comments Inorg. Chem.*, 1988, 237.
20 L. R. Gahan, T. W. Hambley, A. M. Sargeson and M. R. Snow, *Inorg. Chem.*, 1982, **21**, 2699.
21 W. Clegg, *Acta Crystallogr., Sect. A*, 1981, **37**, 22.
22 SHELX 76, program for crystal structure refinement, G. M. Sheldrick, University of Cambridge, 1976.
23 D. T. Cromer and J. B. Mann, *Acta Crystallogr., Sect. A*, 1968, **24**, 321.
24 CALC, program for molecular geometry calculations, R. O. Gould and P. Taylor, University of Edinburgh, 1985.
25 ORTEP II, interactive version, P. R. Mallinson and K. W. Muir, *J. Appl. Crystallogr.*, 1985, **18**, 51.

Received 3rd *June* 1994; *Paper* 4/03329I